HHS Public Access

Author manuscript

J Biomech. Author manuscript; available in PMC 2019 August 28.

Published in final edited form as:

J Biomech. 2015 January 02; 48(1): 171–175. doi:10.1016/j.jbiomech.2014.11.005.

Dynamic Nanomechanics of Individual Bone Marrow Stromal Cells and Cell-Matrix Composites during Chondrogenic Differentiation

BoBae Lee[a,1], **Lin Han**[b,1], **Eliot H. Frank**[c], **Alan J. Grodzinsky**[c,d,e,f,*], **Christine Ortiz**[a,*]

[a]Department of Materials Science and Engineering, Massachusetts Institute of Technology, 77 Massachusetts Avenue, Cambridge MA 02139

[b]School of Biomedical Engineering, Science and Health Systems, Drexel University, 3141 Chestnut Street, Philadelphia, PA 19104

[c]Center for Biomedical Engineering, Massachusetts Institute of Technology, 77 Massachusetts Avenue, Cambridge MA 02139

[d]Department of Electrical Engineering and Computer Science, Massachusetts Institute of Technology, 77 Massachusetts Avenue, Cambridge MA 02139

[e]Department of Mechanical Engineering, Massachusetts Institute of Technology, 77 Massachusetts Avenue, Cambridge MA 02139

[f]Department of Biological Engineering, Massachusetts Institute of Technology, 77 Massachusetts Avenue, Cambridge MA 02139

Abstract

Dynamic nanomechanical properties of bovine bone marrow stromal cells (BMSCs) and their newly synthesized cartilage-like matrices were studied at nanometer scale deformation amplitudes. The increase in their dynamic modulus, $|E^*|$ (e.g., 2.4 ± 0.4 kPa at 1 Hz to 9.7 ± 0.2 kPa at 316 Hz at day 21, mean ± SEM), and phase angle, δ, (e.g., 15 ± 2° at 1 Hz to 74 ± 1° at 316 Hz at day 21) with increasing frequency were attributed to the fluid flow induced poroelasticity, governed by both the newly synthesized matrix and the intracellular structures. The absence of culture duration dependence suggested that chondrogenesis of BMSCs had not yet resulted in the formation of a well-organized matrix with a hierarchical structure similar to cartilage. BMSC-matrix composites products demonstrated different poro-viscoelastic frequency-dependent mechanical behavior and energy dissipation compared to chondrocyte-matrix composites due to differences in matrix molecular constituents, structure and cell properties. This study provides important insights into

*Correspondence and requests for materials should be addressed to: Dr. Christine Ortiz, Phone: (617)452-3084, Fax: (617)258-6936, cortiz@mit.edu. Dr. Alan J. Grodzinsky, Phone: (617)253-4969, Fax: (617)258-5239, alg@mit.edu.

[1]denotes equal contribution.

Conflict of interest statement

The authors affirm that they have no financial affiliation or involvement with any commercial organization that has direct financial interest in any matter included in this manuscript.

the design of optimal protocols for tissue-engineered cartilage products using chondrocytes and BMSCs.

Keywords

cartilage; tissue-engineering; bone marrow stromal cells; nanomechanics; poroelasticity

1. Introduction

During the past decade, various nanomechanical approaches have been used to understand the mechanical integrity of individual primary chondrocytes and chondrocytes associated with pericellular matrices, including compression (Koay et al., 2008), indentation (Darling et al., 2010; Darling et al., 2006; Sanchez-Adams et al., 2013; Wilusz et al., 2013), shear (Ofek et al., 2010) and tension (Trickey et al., 2004). These studies laid the ground on how biomechanical signals play a major role in chondrocyte gene expression and biosynthesis. Besides chondrocytes, bone marrow stromal cells (BMSCs) were recently evidenced as a promising alternative cell source for cartilage tissue repair (Mauck et al., 2006). When seeded within a variety of tissue engineering scaffolds and subjected to chondrogenic factors, BMSCs can undergo chondrogenesis within a few days, and produce PCMs mainly composed of types II and VI collagen, aggrecan and other macromolecules found in articular cartilage (Kopesky et al., 2010a). Aggrecan molecules synthesized in vitro by BMSCs harvested from immature and adult equines have significantly longer glycosaminoglycan (GAG) chains and higher nano-compressive stiffness than aggrecan synthesized by chondrocytes (Kopesky et al., 2010a; Lee et al., 2010b).

As previous studies have focused on the biochemical composition and elastic-like tissue-level mechanics of the BMSC-synthesized neo-cartilage matrices (Connelly et al., 2007; Kopesky et al., 2010b), little is known about the dynamic nanomechanical properties of individual cells. Similar to chondrocyte-associated matrix, the BMSC-associated matrix provides important functions in cell signaling and mechanotransduction (Millward-Sadler et al., 2000; Potier et al., 2010) in both static and dynamic loadings. Knowledge of the dynamic nanomechanical properties of the BMSC-matrix composites will provide a critical measure of the potential success of BMSC-based cartilage tissue engineering (Han et al., 2011b). Here, we adapted the atomic force microscopy (AFM)-based dynamic oscillatory nanoindentation (Han et al., 2011a) to assess the dynamic mechanical properties of individual BMSC-matrix composites. The dependence on dynamic frequency and culture duration was investigated to study the poro-viscoelastic properties of this composite, and its cultural time-dependent evolution. The results were compared to our previously study of chondrocyte-matrix composites (Lee et al., 2010a) to highlight the differences in engineered products from these two cell sources.

2. Materials and Methods

2.1 Cell culture and isolation

Bovine BMSCs were isolated and seeded into 2% alginate hydrogel beads at 20×10^6 cells/mL density, similar to the culture of chondrocytes (Ng et al., 2007). The beads were placed in chondrogenic culture medium containing high-glucose DMEM supplemented with 1% Insulin-Transferrin-Selenium (Sigma-Aldrich, St. Louis, MO), 100 nM dexamethasone (Sigma-Aldrich) and 10 ng/mL recombinant human transforming growth factor-β1 (R&D System, Minneapolis, MN) (Connelly et al., 2008). Culture medium was replaced every other day. Groups of BMSCs with their neo-matrices were released from the alginate beads on days 7, 14, and 21 and maintained in high-glucose DMEM for subsequent measurements.

2.2 AFM-based dynamic oscillatory test

Aided by an optical microscope attached to an AFM, individual BMSCs or BMSC-matrix composites were positioned within micro-fabricated inverted pyramidal silicon wells (Fig. 1a) (Ng et al., 2007). Following previous procedures (Lee et al., 2010a), a Multimode Nanoscope IV AFM with a PicoForce piezo (BrukerNano, Santa Barbara, CA) and an electronic wave generator (Rockland 5100, Victoria, British Columbia, Canada) were used to perform dynamic oscillatory indentation on individual cells using a ≈ 5 nm dynamic oscillation amplitude superimposed on a ≈ 1 μm static indentation depth at dynamic frequencies, f (1 – 316 Hz), via spherical silica colloidal probe tips (R_{tip} ≈ 2.5 μm, #SS06N, Bang Labs; tipless cantilever, NP-020, k ≈ 0.06 N/m, BrukerNano). For each time point, we tested $n \geq 10$ cells from $N = 3$ animals, the data were pooled since we did not detect significant differences across animals ($p > 0.05$ via one-way ANOVA).

The resulting dynamic indentation force, F^*, displacement amplitude, D^*, and phase angle of the force to the displacement, δ, were calculated for each test using a previously developed calibration algorithm (Han et al., 2011a). The dynamic indentation modulus, $|E^*|$, was calculated using a Taylor expansion of the elastic Hertz model (Mahaffy et al., 2004),

$$F^* = 2\frac{|E^*|}{\left(1-\nu^2\right)}R^{1/2}D_0^{1/2}D^*,$$

where D_0 is the static indentation depth, ν is the Poisson's ratio, and R is the reduced contact radius (i.e., $1/R = [(1/R_{tip}) + (1/R_{cell\text{-}matrix\ composite})]$). In addition, to quantify the mechanical properties of individual cells, dynamic nanomechanical properties of freshly isolated BMSCs and knee cartilage chondrocytes of the same-aged calves were measured on day 0, prior to seeding into an alginate gel, and therefore, prior to the development of cell-associated matrices. For all the tests, $\nu \approx 0.4$ measured on chondrocytes (Freeman et al., 1994) was used. For the PCM, though it was reported $\nu \approx 0.04$ (Alexopoulos et al., 2005), the effects of ν on $|E^*|$ (≈ 15% over $\nu = 0.04$ to 0.4) do not affect our major conclusions.

2.3 Statistical tests

For individual BMSCs, chondrocytes, and BMSC-matrix composites, the effects of dynamic frequency on $|E^*|$ and δ were tested via one-way ANOVA, followed by Tukey-Kramer post-

hoc tests. For the BMSC-matrix composites, their dependence on culture duration was tested via least squares linear regression (LSLR) at each frequency. Comparison of $|E^*|$ and δ between individual BMSCs and chondrocytes was carried out via student's t-test. In all the tests, $p < 0.05$ was taken as statistical significant.

2.4 Histological and biochemical analyses

The total amounts of collagen and sulfated GAGs per DNA (as a measure of cell number) within the BMSC-matrices were assessed via dimethylmethylene blue dye binding (Farndale et al., 1986) and hydroxyproline (Woessner, 1961) assays, respectively. Histology of individual cell-matrix composite was also performed using toluidine blue to stain for sulfated PGs and aniline blue to stain for collagen, respectively, following previous procedures (Ng et al., 2007).

3. Results

For all BMSC-matrix composites measured, both $|E^*|$ and δ increased significantly with increasing dynamic frequency from 1 – 316 Hz (one-way ANOVA, $p < 0.0001$, Fig. 1b,c). In this experiment, the static indentation depth (≈ 1 μm) is ≈ 10% of the total diameter of the cell-matrix composite (≈ 16.4 μm). In addition, linear dependences of $|E^*|$ versus $f^{1/2}$ were observed for the composites at all culture days ($R^2 > 0.81$ via LSLR, Fig. 1d). Over the 21 days of culture, we did not observe significant trends in $|E^*|$ or δ with culture duration (Fig. 1b,c), as no significant slope was found for $|E^*|$ or δ versus culture days via LSLR.

Similar frequency dependence of $|E^*|$ and δ was also observed for both BMSCs and chondrocytes prior to the culture (without the associated matrices, Fig. 2a). While $|E^*|$ was similar for both cells types up to 100 Hz (Fig. 2a), BMSC showed significantly higher δ at all tested frequencies except for 100 Hz (Fig. 2b, unpaired two-sample t-test, *: $p < 0.05$). A higher degree of linear dependence of $|E^*|$ versus $f^{1/2}$ was observed for chondrocytes ($R^2 > 0.82$, Fig. 2a), but not for BMSCs ($R^2 < 0.63$).

In histological staining, sulfated GAGs (mostly on aggrecan) and collagen were observed in the newly developed matrix after 21 days culture (Fig. 3a). Similarly, biochemical assays showed increased collagen and GAGs during culture (Fig. 3b), confirming that BMSCs underwent chondrogenesis and synthesized cartilage-like matrices similar to chondrocytes (Ng et al., 2007).

4. Discussion

4.1 Poro-viscoelasticity of BMSC-matrix composites

The significant frequency dependence of $|E^*|$ and δ (Fig. 1) suggested the dominance of time-dependent poro-viscoelasticity of BMSC-matrix composites. Since the static indentation is ≈ 25% of the neo-matrices, this frequency dependence likely involves contributions from both the matrix and intracellular structures. Poroelasticity is thus originated from fluid flow through both the cytoskeletal filaments and organelles within the cell (Charras et al., 2005), and the negatively charged aggrecan in the newly synthesized matrix (Mow et al., 1980). In our experimental set-up, poroelastic energy dissipation is

expected to increase with frequency because the characteristic poroelastic frequency, f_p, is ~ 100Hz ($f \leq f_p$). The value of f_p is estimated based on $f_p \sim Hk/L^2$ (Mow et al., 1980), where the aggregate modulus $H \sim 0.1$ kPa (Lee et al., 2010a), hydraulic permeability $k \sim 10^{-12} m^4 \cdot N^{-1} \cdot s^{-1}$ (Eisenberg and Grodzinsky, 1988), and the fluid flow length scale $L \sim 1$ μm. Viscoelasticity is the combined effects of the macromolecular friction between collagen, aggrecan, and intracellular BMSC cytoplasm constituents. At this nm-scale deformation amplitude and within this frequency domain, we expect poroelasticity to dominate, as evidenced in the linear dependence of $|E^*|$ versus $f^{1/2}$ (Fig. 1d). This linear dependence is similar to the response of both chondrocyte-matrix composite (Lee et al., 2010a), and native cartilage (Han et al., 2011a). The absence of culture day dependence likely suggested that chondrogenesis had not yet resulted in the formation of a well-organized matrix with a hierarchical structure similar to cartilage ECM. The native ECM is mainly composed of crosslinked collagen network entrapping densely packed aggrecan (Maroudas, 1979). Thus, hydraulic permeability of this immature matrix is comparably high, and the associated poro/viscoelastic resistance to indentation load was not yet developing rapidly to yield a change up to 21 days of alginate culture.

4.2 Poro-visoelasticity of individual BMSCs

Interestingly, when performing these tests on individual chondrocytes in the absence of neomatrices, we observed similar linear dependence of $|E^*|$ and $f^{1/2}$ on chondrocytes (Fig. 2a). The similarity in the dynamic mechanics of isolated chondrocytes (Fig. 2a), chondrogenic BMSC-matrix composites (Fig. 1d) and chondrocyte-matrix composites (Lee et al., 2010a), and native cartilage (Han et al., 2011a) could be important for the deformation properties of these hierarchical, connected structures of cartilage during joint loading, and in turn affect the mechano-transduction of cells (Millward-Sadler et al., 2000). In comparison, without undergoing chondrogenesis, such linear dependence is absent for individual BMSCs (Fig. 2a), which suggests that poroelastic-like energy dissipation mechanisms lag in development behind those of chondrocytes, since added time is needed for the processes of differentiation and maturation of BMSC-seeded constructs.

4.3 Comparison with chondrocyte-matrix composites

In order to further elucidate the biosynthetic activities of BMSCs, we compared the BMSC-matrix composite nanomechanical properties with our previously reported chondrocyte-matrix composites synthesized in the absence of growth factors, similar to this study (Fig. 4). For these two cell types, we observed marked differences in both biochemical and biomechanical properties. At day 21 of culture, the accumulation of aggrecan and collagen in BSMCs is ≈ 50% of that in chondrocyte-alginate culture (Fig. 4a), partly due to the fact that it takes ~3–7 days for the initiation of chondrogenic differentiation of BMSCs (Kopesky et al., 2010a). Interesting, despite much less collagen and aggrecan present in the matrix, at lower frequency (1 Hz), BMSC-matrix composites showed similar $|E^*|$ and greater elasticity (lower δ) compared to the chondrocyte-matrix composites. This observation can be attributed to the superior ultrastructure and nanomechanical properties of aggrecan monomers synthesized by BMSCs compared to those by chondrocytes (Kopesky et al., 2010a; Lee et al., 2010b), leading to relatively enhanced, more elastic mechanical properties. In contrast, at the highest tested frequency, $f = 316$ Hz (Fig. 4b,c), the BMSC-matrix

composites showed significantly lower $|E^*|$ and greater viscous deformation (higher δ) than that for the chondrocyte-matrix composites. This is most likely due to the higher matrix k of the less solid-like matrix given the lower aggrecan and collagen content.

5. Conclusions

In this study, we quantified the dynamic nanomechanical properties of individual BMSCs and their associated tissue-engineered matrices. The non-linear frequency dependence was mainly attributed to fluid-flow induced poroelastic energy dissipation. In addition, despite increase in collagen and GAG contents in the PCM during culture, there was a lack of culture duration dependence for both $|E^*|$ and δ, suggesting a delay in the formation of hierarchical structure of the matrix similar to native cartilage. The distinct differences in dynamic mechanical properties of chondrocyte- and BMSC-matrix composites may result in discrepancies in cell signaling and mechanostransduction and affect the ultimate outcome of the tissue-engineered product. Ongoing studies will probe the submicron-meter ultrastructure of the BMSC-associated matrix, as well as the dynamic responses at higher frequencies and longer culture duration to obtain more insights into the protocol of cartilage tissue-engineering via BMSCs.

Acknowledgements

We thank the Institute for Soldier Nanotechnologies at MIT, funded through the U.S. Army Research Office, for use of instruments. This work was supported by National Science Foundation (grant CMMI-0758651), the National Institutes of Health (grant AR033236), the National Security Science and Engineering Faculty Fellowship (grant N00244–09-1–0064) and the Faculty Start-up Grant at Drexel University (LH).

References

Alexopoulos LG, Williams GM, Upton ML, Setton LA, Guilak F, 2005 Osteoarthritic changes in the biphasic mechanical properties of the chondrocyte pericellular matrix in articular cartilage. J. Biomech 38, 509–517. [PubMed: 15652549]

Charras GT, Yarrow JC, Horton MA, Mahadevan L, Mitchison TJ, 2005 Non-equilibration of hydrostatic pressure in blebbing cells. Nature 435, 365–369. [PubMed: 15902261]

Connelly JT, Garcia AJ, Levenston ME, 2007 Inhibition of in vitro chondrogenesis in RGD-modified three-dimensional alginate gels. Biomaterials 28, 1071–1083. [PubMed: 17123602]

Connelly JT, Wilson CG, Levenston ME, 2008 Characterization of proteoglycan production and processing by chondrocytes and BMSCs in tissue engineered constructs. Osteoarthritis Cartilage 16, 1092–1100. [PubMed: 18294870]

Darling EM, Wilusz RE, Bolognesi MP, Zauscher S, Guilak F, 2010 Spatial mapping of the biomechanical properties of the pericellular matrix of articular cartilage measured in situ via atomic force microscopy. Biophys. J 98, 2848–2856. [PubMed: 20550897]

Darling EM, Zauscher S, Guilak F, 2006 Viscoelastic properties of zonal articular chondrocytes measured by atomic force microscopy. Osteoarthritis Cartilage 14, 571–579. [PubMed: 16478668]

Eisenberg SR, Grodzinsky AJ, 1988 Electrokinetic micromodel of extracellular matrix and other polyelectrolyte networks. PhysicoChem. Hydrodyn 10, 517–539.

Farndale RW, Buttle DJ, Barrett AJ, 1986 Improved quantitation and discrimination of sulfated glycosaminoglycans by use of dimethylmethylene blue. Biochim. Biophys. Acta 883, 173–177. [PubMed: 3091074]

Freeman PM, Natarajan RN, Kimura JH, Andriacchi TP, 1994 Chondrocyte cells respond mechanically to compressive loads. J. Orthop. Res 12, 311–320. [PubMed: 8207584]

Han L, Frank EH, Greene JJ, Lee H-Y, Hung H-HK, Grodzinsky AJ, Ortiz C, 2011a Time-dependent nanomechanics of cartilage. Biophys. J 100, 1846–1854. [PubMed: 21463599]

Han L, Grodzinsky AJ, Ortiz C, 2011b Nanomechanics of the cartilage extracellular matrix. Annu. Rev. Mater. Res 41, 133–168. [PubMed: 22792042]

Koay EJ, Ofek G, Athanasiou KA, 2008 Effects of TGF-beta 1 and IGF-I on the compressibility, biomechanics, and strain-dependent recovery behavior of single chondrocytes. J. Biomech 41, 1044–1052. [PubMed: 18222457]

Kopesky PW, Lee H-Y, Vanderploeg EJ, Kisiday JD, Frisbie DD, Plaas AHK, Ortiz C, Grodzinsky AJ, 2010a Adult equine bone marrow stromal cells produce a cartilage-like ECM mechanically superior to animal-matched adult chondrocytes. Matrix Biol. 29, 427–438. [PubMed: 20153827]

Kopesky PW, Vanderploeg EJ, Sandy JS, Kurtz B, Grodzinsky AJ, 2010b Self-assembling peptide hydrogels modulate in vitro chondrogenesis of bovine bone marrow stromal cells. Tissue Eng. A 16, 465–477.

Lee B, Han L, Frank EH, Chubinskaya S, Ortiz C, Grodzinsky AJ, 2010a Dynamic mechanical properties of the tissue-engineered matrix associated with individual chondrocytes. J. Biomech 43, 469–476. [PubMed: 19889416]

Lee H-Y, Kopesky PW, Plaas AHK, Sandy JD, Kisiday J, Frisbie D, Grodzinsky AJ, Ortiz C, 2010b Adult bone marrow stromal cell-based tissue-engineered aggrecan exhibits ultrastructure and nanomechanical properties superior to native cartilage. Osteoarthritis Cartilage 18, 1477–1486. [PubMed: 20692354]

Mahaffy RE, Park S, Gerde E, Kas J, Shih CK, 2004 Quantitative analysis of the viscoelastic properties of thin regions of fibroblasts using atomic force microscopy. Biophys. J 86, 1777–1793. [PubMed: 14990504]

Maroudas A, 1979 Physicochemical properties of articular cartilage, in: Freeman MAR (Ed.), Adult Articular Cartilage. Pitman, England, pp. 215–290.

Mauck RL, Yuan X, Tuan RS, 2006 Chondrogenic differentiation and functional maturation of bovine mesenchymal stem cells in long-term agarose culture. Osteoarthritis Cartilage 14, 179–189. [PubMed: 16257243]

Millward-Sadler SJ, Wright MO, Davies LW, Nuki G, Salter DM, 2000 Mechanotransduction via integrins and interleukin-4 results in altered aggrecan and matrix metalloproteinase 3 gene expression in normal, but not osteoarthritic, human articular chondrocytes. Arthritis Rheum. 43, 2091–2099. [PubMed: 11014361]

Mow VC, Kuei SC, Lai WM, Armstrong CG, 1980 Biphasic creep and stress relaxation of articular cartilage in compression: theory and experiments. J. Biomech. Eng 102, 73–84. [PubMed: 7382457]

Ng L, Hung H-H, Sprunt A, Chubinskaya S, Ortiz C, Grodzinsky A, 2007 Nanomechanical properties of individual chondrocytes and their developing growth factor-stimulated pericellular matrix. J. Biomech 40, 1011–1023. [PubMed: 16793050]

Ofek G, Dowling EP, Raphael RM, McGarry JP, Athanasiou KA, 2010 Biomechanics of single chondrocytes under direct shear. Biomech. Model. Mechanobiol 9, 153–162. [PubMed: 19644718]

Potier E, Noailly J, Ito K, 2010 Directing bone marrow-derived stromal cell function with mechanics. J. Biomech 43, 807–817. [PubMed: 19962149]

Sanchez-Adams J, Wilusz RE, Guilak F, 2013 Atomic force microscopy reveals regional variations in the micromechanical properties of the pericellular and extracellular matrices of the meniscus. J. Orthop. Res 31, 1218–1225. [PubMed: 23568545]

Trickey WR, Vail TP, Guilak F, 2004 The role of the cytoskeleton in the viscoelastic properties of human articular chondrocytes. J. Orthop. Res 22, 131–139. [PubMed: 14656671]

Wilusz RE, Zauscher S, Guilak F, 2013 Micromechanical mapping of early osteoarthritic changes in the pericellular matrix of human articular cartilage. Osteoarthritis Cartilage 21, 1895–1903. [PubMed: 24025318]

Woessner JF, 1961 The determination of hydroxyproline in tissue and protein samples containing small proportions of this imino acid. Arch. Biochem. Biophys 93, 440–447. [PubMed: 13786180]

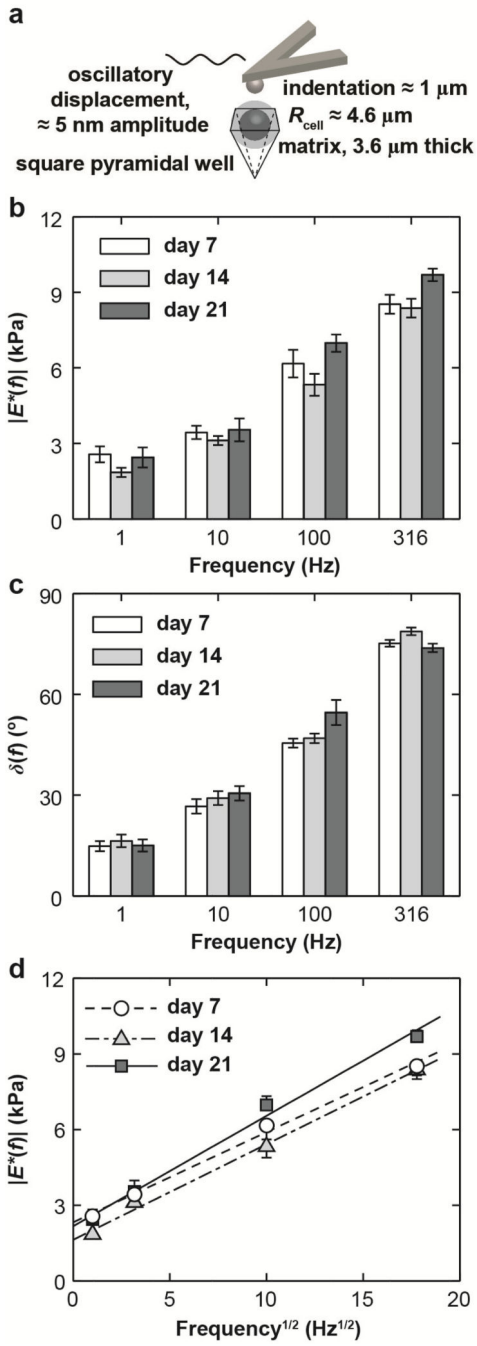

Fig. 1.

(a) Schematic of AFM-based dynamic oscillatory nanoindentation on BMSC-matrix composites in a pyramidal silicon well via a spherical tip ($R_{tip} \approx 2.5$ μm) in PBS. (b) Dynamic complex modulus $|E^*|$ and (c) phase angle, δ, of BMSC-matrix composites as a function of frequency, f, at 7, 14 and 21 days of culture. (d) Least squares linear regression of $|E^*|$ versus $f^{1/2}$ for BMSC-matrix composites at all three culture days, where dashed lines were the regression fits, $R^2 \geq 0.81$. ($n \geq 10$ cells, mean ± SEM for (b-d)).

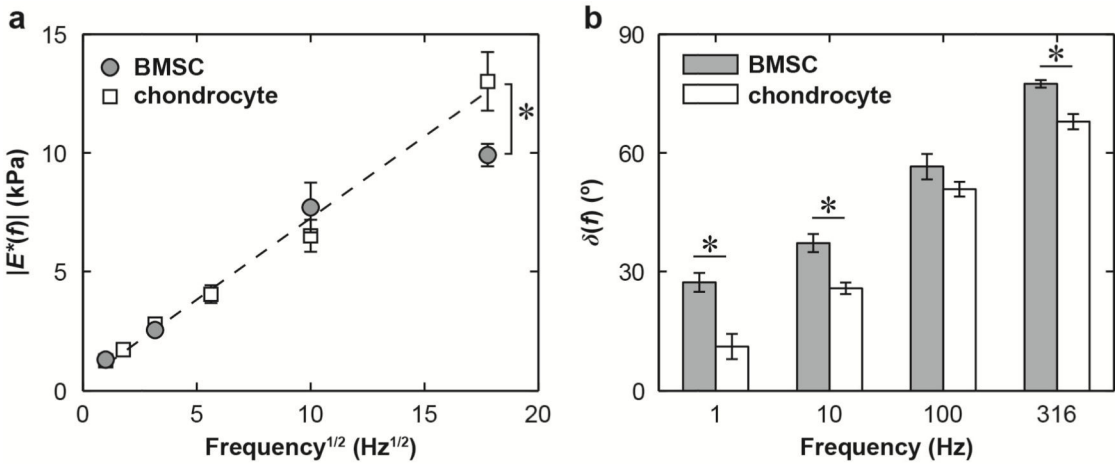

Fig. 2.

Dynamic nanomechanical properties of the BMSCs and chondrocytes at day 0 in PBS, without associated matrices. (a) Least squares linear regression of dynamic modulus, $|E^*|$, as a function of the square root of dynamic frequency, $f^{1/2}$, where dashed line wass the regression fit for chondrocytes ($R^2 \geq 0.82$), while no strong linear dependence was found for the BMSCs ($R^2 < 0.63$). (b) Phase angle, δ, as a function of f ($n \geq 10$ cells, mean ± SEM). *: $p < 0.05$ between BMSCs and chondrocytes via student's t-test at each frequency.

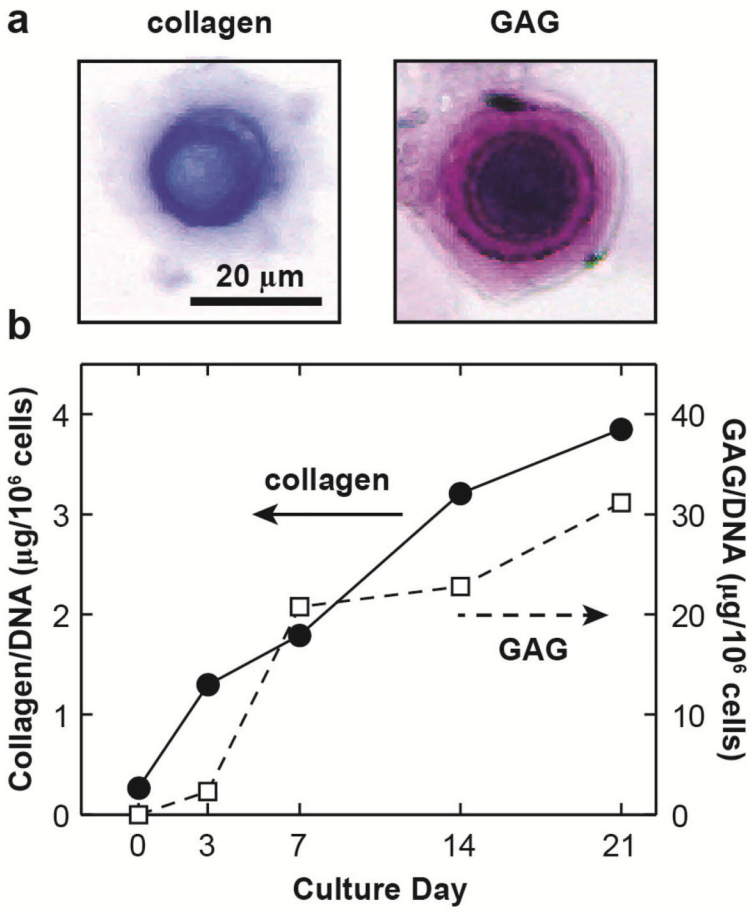

Fig. 3.

(a) Optical microscopy images of individual bovine BMSC-matrix composites after 21 days of culture, stained for collagen and glycosaminoglycan (GAG). (b) Total amounts of collagen and GAG within the newly synthesized matrix by bovine BMSCs at different culture days in fetal bovine serum (FBS).

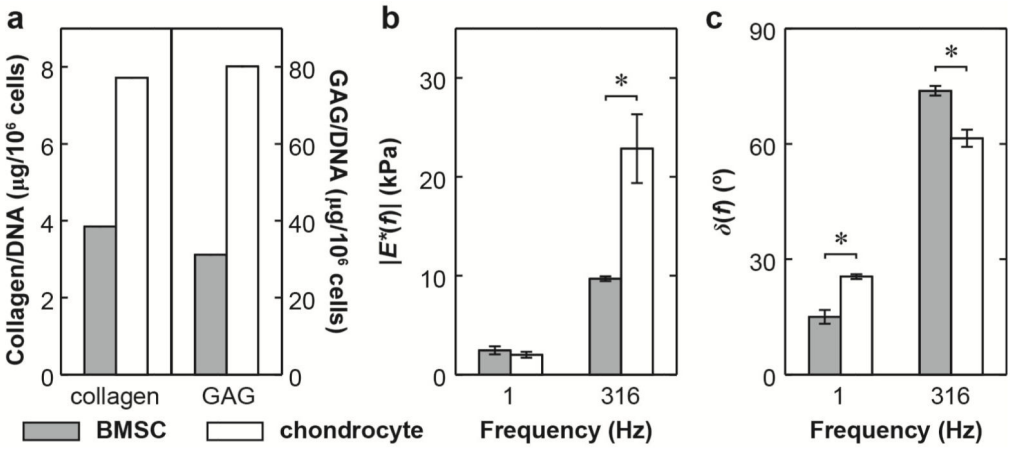

Fig. 4.

Comparison of biochemical and nanomechanical properties of BMSC- and chondrocyte-associated matrix composites at 21 days of culture in fetal bovine serum (FBS). (a) Total amounts of collagen and GAGs within the newly synthesized matrix. (b) Dynamic modulus, $|E^*|$, (c) phase angle, δ, of BMSC-matrix and chondrocyte-matrix composites at $f = 1$ and 316 Hz: ($n \geq 10$ cells for BMSCs, and $n \geq 5$ cells for chondrocytes, mean ± SEM). Data for chondrocytematrix composites are adapted from (Lee et al., 2010a). *: $p < 0.05$ via student's *t*-test at each frequency.